

ADVANCES IN THE DEVELOPMENT OF POLYMERIC FIBERS WITH HIGH ELASTIC ENERGY STORAGE CAPACITY

Hassan Mahfuz¹ and Mujibur R. Khan²

¹Ocean & Mechanical Engineering Department, Florida Atlantic University, Boca Raton, FL 33431

²Department of Mechanical Engineering, University of Texas at El Paso, El Paso, Texas 79968

ABSTRACT

Polymer fibers such as Nylon, Polyester, Polyethylene, Kevlar, and Spectra have wide range of industrial applications which go beyond the realm of traditional composites. From light weight armor to automotive bumpers, tires, air bags, to drug delivery, tissue engineering to wound dressing, polymeric fibers have ever increasing demands. In most of these applications, the elastic energy storage capacity, Ω of these fibers would be an important parameter to gauge their performances. The cubic root of Ω , i.e., ${}^3\sqrt{\Omega}$, also known as normalized velocity of the fiber essentially determines as to how much energy can be stored [1-3]. That

is:

$${}^3\sqrt{\Omega} = \left(\frac{\sigma_{y\max} \varepsilon_{y\max}}{2\rho_y} \sqrt{\frac{E_y}{\rho_y}} \right)^{1/3}$$

where $\sigma_{y\max}$, $\varepsilon_{y\max}$, ρ_y and E_y are strength, fracture strain, density, and modulus of the fiber, respectively

It is obvious that to enhance fiber performance, one has to increase $\sigma_{y\max}$, $\varepsilon_{y\max}$, E_y and reduce ρ_y .

Normalized velocities for commercial fibers such as Nylon-6, Spectra, Kevlar, and Dyneema lie between 500 and 800 m/sec. To revolutionize energy absorption and dissipation, ${}^3\sqrt{\Omega}$ must be doubled, tripled, or even quadrupled. Nanoparticle reinforcement and polymer hybridization offer a unique opportunity to accomplish such goals. The strength and modulus of Nylon – a polyamide based fiber, is one order lower than that of Spectra – a polyethylene based fiber. On the other hand, fracture strain of Nylon is one order higher than that of Spectra. Molecular structures of Nylon and Spectra are such that one provides higher elongation while the other contributes to strength and modulus. If these two polymers can be blended into one precursor, fibers with very high elastic energy will be a reality. From quantum energy concept, this exchange of molecular features is possible since both polymers transition from liquid to solid over a wide range of temperatures allowing an opportunity to exchange such features. However, blending alone will not be enough to increase normalized velocity; hence infusion of CNTs is also considered. This strategy of coupling nanoscale inclusion with polymer blending is expected to increase ${}^3\sqrt{\Omega}$ substantially. In this investigation, we have blended Nylon-6 with ultrahigh molecular weight polyethylene (UHMWPE) to develop a hybrid polymer precursor. To enhance strength and modulus further, we have infused single-walled carbon nanotubes (SWCNTs) into the blended polymer. In the three phase system, the loading of UHMWPE, Nylon 6 and SWCNT was 78 wt%, 20 wt% and 2 wt%, respectively. Hybridized fibers were processed using a solution spinning method coupled with melt mixing and extrusion. A phenomenal increase in strength, modulus, and fracture strain of UHMWPE fiber by 103%, 219%, and 108%, respectively was observed. This processing also resulted in 441% and 88% increase in toughness and normalizing velocity. Nylon 6 in the blend increased intercrystalline amorphism inducing plasticity, while SWCNTs shared the load and co-continuously deformed – both contributing to the improvement that we have observed. Differential scanning calorimetry (DSC), x-ray diffraction (XRD), and scanning electron microscopy (SEM) studies have shown that changes in percent crystallinity, rate of crystallization, crystallite size, alignment of nanotubes, and sliding at the interfaces were responsible for such enhancement. Details of fiber processing, thermal and mechanical characterizations and elastic energy evaluation are described in the paper.

Keywords: UHMWPE, Nylon 6, SWCNT, Hybridizing, Solution Spinning, Toughness

1. INTRODUCTION

Over the last several years researchers have successfully dispersed carbon nanotubes into thermoplastic polymers demonstrating that strength and modulus could be improved significantly [4-10]. However, those improvements were achieved with a significant loss in fracture strain, which eventually decreased the energy absorption capacity in the 30-50% range. On the other hand, research on low density polyethylene (LDPE) has revealed that dispersing a second polymer phase can improve the fracture strain and toughness [11] of the matrix polymer. It is therefore believed that if UHMWPE can be hybridized with Nylon 6, one would be able to increase fracture strain significantly. Since these two polymers are immiscible, there is a poor transfer of force between the two phases. Two steps were undertaken to overcome this problem. In our case nylon was designed as the minor phase. Ultrasonic cavitation and homogenization was used to break the spherical domains of the minor phase into smaller droplets. These droplets could elongate into an ellipsoid and control the load transfer depending on the interfacial adhesion between the two phases. We also used an anti-oxidant to work as a reactive compatibilizer to enhance such interfacial adhesion. It is expected that compatibilizer will reduce interfacial tension resulting in reduction in the size of the dispersed (minor) phase, and it will also enhance interfacial adhesion through the formation of micro-bridges. The fine nylon phase thus coupled to the main phase (UHMWPE) in compatibilized blends would carry load and deform simultaneously. This would allow large yielding and high fracture strain of the blended fiber.

Although compatibilizer would allow polymer blends to have large fracture strain, the resulting strength and modulus would be somewhat intermediate between the two blended polymers. To enhance strength and modulus substantially higher than that of the blended polymer, we infused SWCNTs in the polymer blend prior to spinning. Solution spinning and melt mixing enforce interaction between SWCNTs and polymer molecules. Especially, as amide link opens up during polymerization, it would give an opportunity for SWCNTs to interact with nylon through dipole-ion interaction. SWCNTs embedded between two polymer phases (major and minor) would facilitate interface sliding, and deform both axially and transversely, providing excellent mechanisms to enhance toughness and modulus.

2. EXPERIMENTAL PROCEDURES

Commercial grade UHMWPE powder, paraffin oil and anti-oxidant (2, 6-di-t-butyl, 4- methylcresol) and SWCNTs were procured from Sigma Aldrich (6000 North Teutonia Ave. Milwaukee, WI 53209). The average density, melting point and molecular weight of UHMWPE were 0.94 g/cm³, 138 °C and 3x10⁶ g/mole, respectively. SWCNTs were 2-10 nm in diameter and were approximately 1-2 μm long. SWCNTs were not functionalized with any chemical group. Nylon 6 was procured from UBE Industries, Ltd (UBE building 3-11

Higashi-shinagawwa 2 chome, Shinaga-wa-Ku, Tokyo 140, Japan). Average density, melting point, and molecular weight of nylon 6 were 1.14 g/cm³, 220 °C, and 20x10³ g/mole, respectively. All categories of filaments were fabricated using a Laboratory Mixing Extruder (LME). The extrusion apparatus included a coaxial cylinder, a turning rotor heater, an outlet die, an orifice, a hexane bath, an oven, and a filament take up system. Four types of filaments were produced; (1) neat UHMWPE (2) UHMWPE with 20.0 wt% of nylon 6 (3) UHMWPE with 2.0 wt% of SWCNT, and (4) UHMWPE with 20.0 wt % of nylon 6 and 2.0 wt% of SWCNT.

To synthesize neat UHMWPE filaments (type-1), 95.0 wt% of paraffin oil was mixed with 5.0 wt% of UHMWPE using a VDI-25 homogenizer. After mixing for about 15 minutes, the admixture was fed into the LME hopper and passed through the annular zone between the cylinder and the turning rotor. The solution was simultaneously heated to 150 °C using the turning rotor. At this stage the solution turned into a viscous gel and as the rotation continued it flowed into the outlet die and exited through a 3mm dia orifice. After extrusion, filaments were rinsed through a hexane bath, passed through a heater (100 °C), and drawn into the take-up spindle (filament winder) with controlled stretching. Hexane was used to extract paraffin oil from the gelled filament as it came out of the extruder. After filaments were collected in the filament winder, they were cut into strands and subjected to a secondary heating at 60-70 °C in a separate oven for a prolonged period of time (~48 hrs). The secondary heating was necessary to remove residual paraffin oil from the filament.

For type-2 filaments, 94.5 wt% of paraffin oil, 4.0 wt% of UHMWPE, 1.0 wt% of nylon 6, and 0.5 wt% of anti-oxidant (2, 6-di-t-butyl, 4- methylcresol) were mixed using the homogenizer. Filaments were then extruded using the LME at 170 °C and following the procedures stated above. For type-3 filaments, ratio of paraffin oil, UHMWPE, and SWCNTS was 95.0 wt%, 4.9 wt%, and 0.1 wt%, respectively. SWCNTs were first dispersed into paraffin oil using a VCX-500 ultrasonic processor for about an hour. After sonication, UHMWPE was mixed with the solution using the homogenizer. Filaments were then extruded using the previous procedures. In type-4, ratio of paraffin oil, UHMWPE, nylon 6, anti-oxidant, and SWCNTs was 94.5 wt%, 3.92 wt%, 0.98 wt%, 0.5 wt%, and 0.1 wt%, respectively and filaments were produced using steps similar to type-3. Weight percentages mentioned above conform to 20.0 wt% of nylon 6 and 2.0 wt% of SWCNTs as required in respective categories after paraffin oil is removed.

Once the filaments were produced they were tested under tension using a Zwick-Roell material testing machine according to ASTM D3379-75. Diameters of the filaments were measured using a SEM. Tests were run at a constant crosshead speed of 2 mm/min using a 20 N load cell. A gage length of 30 mm was generally used. About 10 individual filaments were tested in each category. DSC, XRD and SEM analysis were carried out to investigate morphology, structure formation, crystal structure and fracture behavior. DSC ramp tests were

carried out under inert atmosphere with a heating and cooling rate of 10°C/min using a TA Q10 DSC apparatus. SEM analyses were performed in a D8303 Quanta 200 scanning electron microscope. X-ray diffraction measurements were conducted using a Siemens D5000 diffractometer equipped with a diffracted beam monochromator, and operating at 45kV, 40mA and Cu-K α radiation.

3. RESULTA AND DISCUSSIONS

3.1 Tensile Tests

Representative stress-strain diagrams and the data from tensile tests are shown in Fig. 1 and Table- 1, respectively. It has been observed that with the addition of nylon 6 (Fig. 1b), the fracture strain of the filament increased by almost 77% without any discernible change in yield strength (0.2% offset), ultimate tensile strength and Young's modulus. On the other hand, with the infusion of SWCNTs (Fig. 1c) the modulus, yield strength and ultimate tensile strength increased by 463%, 450% and 120%, respectively. Extremely high modulus of SWCNTs (~ 1.5 TPa) has contributed to such increases by sharing the load. Moreover, large increase in strength suggests that the presence of a strong affinity between the polymer and the nanotubes. Such interactions can

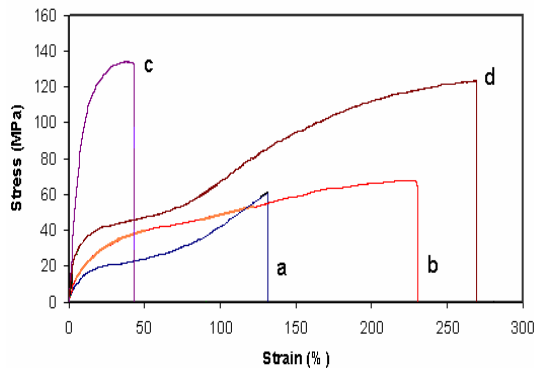


Fig 1. Stress-strain curves of: (a) UHMWPE, Type-1, (b) UHMWPE-Nylon 6, Type-2, (c) UHMWPE-SWCNT, Type-3, (d) UHMWPE-Nylon 6- SWCNTNylon 6, Type-4

significantly restrict polymer's chain mobility. Strain to fracture thus reduced by 68%.

However, with the addition of nylon 6 in SWCNT-reinforced UHMWPE (Fig. 1d), fracture strain increased substantially (108%). It is also observed in Table-1 that yield strengths of type-4 and type-3 filaments are 32 MPa and 110 MPa, respectively. Although the yield strength of type-4 system was lower than that of the type-3, it was still much higher (~ 60%) than that of the neat UHMWPE (type-1) filaments. It is also noticed that the tensile strength of type-4 (Fig 1d) is very close to that of type 3 (Fig. 1c). It is evident in Fig. 1 that different categories of filaments have distinctive pattern in their stress strain response. Figure 1a and 1b show a single stage plateau with moderate increase in strength level while Fig. 1c demonstrates a spiky increase in strength without the presence of any plateau. Failure patterns are also different; former categories (1a and 1b) are indicative of being plastic in nature while the latter (1c) is brittle. On the other hand, curve of 1d, has two distinct plateaus. It suggests that the material yields at an early stage of loading, but strength level continues to increase with increased deformation demonstrating strain hardening capability of the material [12]. Accordingly, we see remarkable increase in strength level during the 2nd plateau.

We calculated modulus of toughness (u_t) from the area under each of the stress-strain curves. The areas were calculated using the Trapezoidal rule and are shown in Table-1. It is observed in Table-1 that the toughness of type-4 filaments increased by 441% compared to that of neat filaments (type-1). This phenomenal increase in toughness was only possible with the inclusion of both nylon 6 and SWCNTs with UHMWPE. When nylon 6 was added (i.e., typ-2), increase in toughness was 180%, and with typ-3 the increase was very nominal – justifying that dual inclusion strategy was necessary to substantially increase the toughness. Next, the normalizing velocities were calculated using the values of σ_{max} , E , ϵ_{max} , and ρ in Table-1. The densities (ρ) of hybridized and nanoparticle reinforced filaments were determined using the rule of mixture. Calculated values of normalizing velocities are listed in Table-1. It is seen that normalizing velocity increased only by 16% with

Table 1 Tensile Test Data

Filament samples	σ_y (MPa)	σ_{max} (MPa)	E (MPa)	ϵ_{max} (%)	ρ (Kg/m ³)	u_t (MJ/m ³)	$^3\sqrt{\Omega}$ (m/s)
Neat UHMWPE (type-1)	20±5	61±6	238±6	130	940	41	277
UHMWPE-Nylon 6 (type-2)	21 ± 5	61 ± 7	240 ±19	230	982	115	328
UHMWPE-SWCNT (type-3)	110 ±10	134±11	1340±21	42	973	48	323
UHMWPE-SWCNT-Nylon 6 (type-4)	32 ±6	124±9	760±6	270	1015	222	522

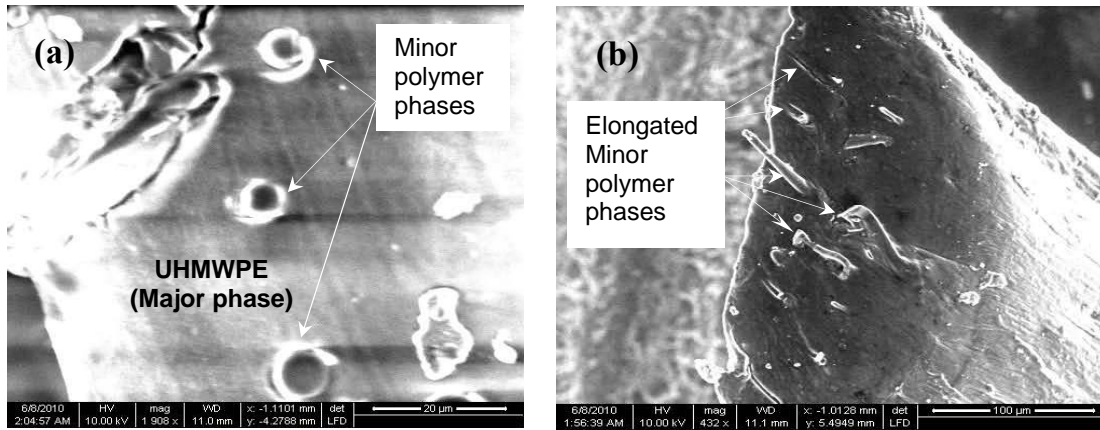


Fig 2. SEM micrographs of UHMWPE-SWCNT-Nylon 6 (a) cross-sectional view of an undeformed filament, (b) Cross-sectional view of a deformed filament

the inclusion of SWCNTs (type-3). Although the increase in strength and modulus was significant, increase in normalizing velocity was very modest because of the reduced fracture strain. However, when nylon 6 was added in the SWCNT reinforced UHMWPE, the normalizing velocity increased by 88%. Such improvement occurred because of the large increase in fracture strain by about 108% as indicated earlier.

3.2 SEM Studies

SEM images of un-deformed and deformed UHMWPE-SWCNT-nylon 6 filaments (cross-sectional view) are shown in Figs 2a and 2b, respectively. Evidence of minor phases as droplets in an extruded filament is shown in Fig 2a. Energy Dispersive X ray Spectroscopy (EDS) analysis has also confirmed these minor phases as nylon. The droplets were around 4-7 μm in diameter and distributed randomly inside the matrix materials (UHMWPE). As-received nylon particles were 15-30 μm in diameter. It is therefore seen that a considerable amount of size reduction of the minor phase has taken place due to blending and extrusion. This reduction in size however is an indication of reduced interfacial tension between the major and minor phases [13]. The cross-sectional view of a deformed UHMWPE-SWCNT-nylon 6 filament is shown in Fig. 2b. This particular filament was stretched up to 180% strain, and elongated minor phases (nylon 6) are quite visible in the micrograph. As the loading continued, the minor phase elongated more and more, but stayed attached to the matrix (major phase). The ability of nylon to stretch allowed the composite to deform plastically as it remained attached to the major phase. As the loading increased, these minor phases began to slide at the interface. This interfacial sliding continued until fracture of the filament occurred. If nanotubes are present, this sliding is prolonged as nanotubes share the load. This issue is discussed later.

3.3 DSC and XRD Analyses

Changes in crystalline morphology due to the nanotubes and polymer inclusion were investigated through DSC and XRD analyses. DSC heating and

cooling curves are shown in Fig. 3 as two curves for each of the three categories of filaments; (a), (b), and (c). Crystallinity and rate of crystallization were determined from the DSC cooling curves in Fig 3. The crystallinity was determined from the area under the cooling exotherms. The crystallization time was also recorded and the rate of crystallization was calculated. DSC results are shown in Table-2. It is observed in Table-2 that crystallinity increased by 22% with SWCNT inclusion. However, with the addition of nylon 6, the crystallinity decreased by 14%. Changes in the rate of crystallization also showed a similar trend. The X-ray diffraction patterns for different categories of samples are shown in Fig 4. The Miller indices for polyethylene, 110 and 200 of the main Bragg peaks are shown in the figure. The diffraction patterns indicate that all categories of samples are partially crystalline. The crystallite size (τ) in the samples was estimated from the full-width at half maximum (FWHM) of the 110 diffraction (2θ) peaks by using the Scherer equation [14, 15]. The Bragg peak (110) angle, FWHM and the calculated values of the crystallite size (τ) are listed in Table-2. The values of τ seem to be slightly higher with SWCNT infusion, whereas a small reduction in crystallite size appears when nylon 6 is added.

In an effort to understand the role of nanotubes, SEM micrographs of extruded filaments were taken as shown in Fig.5. Growth of polymer crystals around the nanotubes is shown by arrows in Fig. 5. Although the dispersed nanotubes were 10-20 nm in diameters, the embedded nanotubes appear to be much larger in size due to the crystal growth surrounding the tubes. Some degree of alignment along the filament length is also evident. Since SWCNTs can act as a strong nucleation agent such crystal growths are common around the nanotubes [16]. UHMWPE, a crystalline polymer therefore aggregated on such nucleation sites and formed hard segments. These hard segments attached to the nanotubes can effectively transfer load to nanotubes while greatly reducing the deformation ability of the polymer. That is why we observed a significant increase in strength but reduction in fracture strain of the UHMWPE when infused with SWCNTs. On the other hand, nylon 6 is

more amorphous in nature compared to UHMWPE. Nylon chains can closely pack and increase intercrystalline amorphous segments. Decrease in crystallinity and crystallite size with the inclusion of nylon 6 (Table-2) also supports this argument. Moreover,

reduction in yield strength and Young's modulus in the three phase system (UHMWPE-SWCNT-nylon 6) compared to those of two phase system (UHMWPE-SWCNT) is the consequence of an increase in the amorphous segments.

Table 2: Results from DSC and XRD tests

Samples	Percent Crystallinity (%)	Rate of crystallization (%/min)	2-Theta (Degrees)	FWHM (Degrees)	Crystallite size, τ (nm)
Neat UHMWPE	33.5	3.4	21.65	0.245	33.0
UHMWPE- SWCNT	55.1	6.45	21.66	0.216	37.4
UHMWPE- SWCNT-nylon 6	41.4	4.48	21.75	0.25	32.3

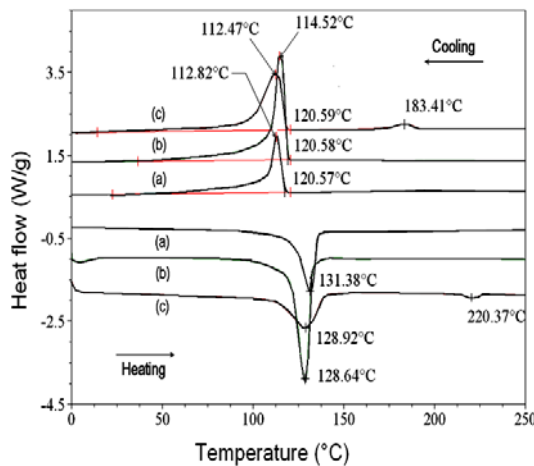


Fig 3. DSC curves of (a) neat UHMWPE (b) UHMWPE-SWCNT and (c) UHMWPE-SWCNT-Nylon 6

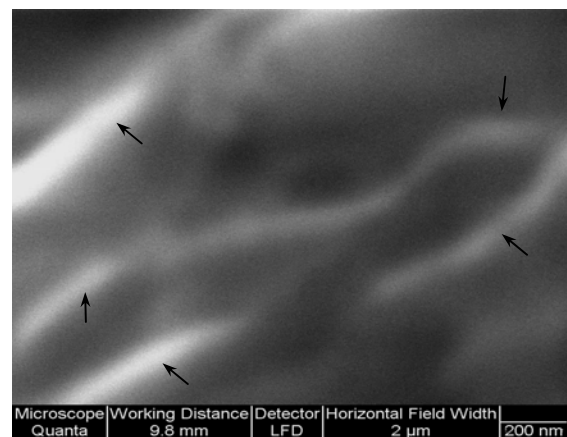


Fig 5. SEM micrograph of the UHMWPE-SWCNT Sample

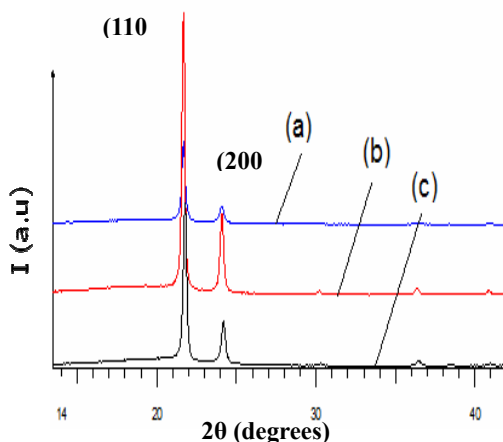


Fig. 4 X-ray diffraction patterns of (a) Neat UHMWPE (b) UHMWPE- SWCNT (c) UHMWPE-SWCNT-Nylon 6.

3.4 Filament Fracture

Fractured surfaces of; (a) UHMWPE-SWCNT and (b) UHMWPE-SWCNT-nylon 6 filaments are shown in Fig. 6. Brittle fracture and fast crack growth are evident in Fig. 6a. The fracture surface is also indicative of a localized and short-lived plastic deformation - presumably during the end of the fracture process as suggested by the stress-strain diagram in Fig. 1c. Three fracture processes that we had observed in our previous studies with nylon and LDPE filaments [11, 17-19] are distinctly absent in this case. On the other hand, when nylon 6 was added in the UHMWPE-SWCNT matrix, the fracture behavior changed significantly. It was observed that considerable lateral contraction (necking) occurred before the final failure. Multiple shear bands generated at various sites inside the material as shown in Fig. 6b which propagated along the filament length (loading direction). Such shear bands are formed due to highly localized shearing strain – in this case caused by sliding between polymer-coated nanotubes and minor phase (nylon 6). This observation supports our earlier assertion that nanotubes assisted in carrying the load as well as contributed to interface

sliding in presence of the minor phase. Neck formation during tensile tests is also a proof of existence of such shear bands. Dispersed minor phase initiated a large number of shear yielded zones throughout the material and SWCNTs acted as slippage sites by sharing the load and promoting sliding between the polymer phases.

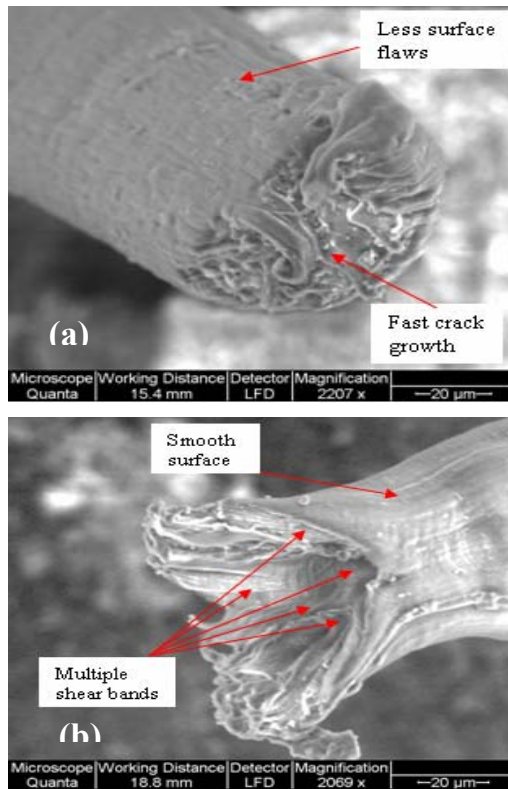


Fig 6. SEM micrographs of fractured surfaces of (a) UHMWPE-SWCNT (b) UHMWPE-SWCNT-Nylon- 6

4. SUMMARY

1. A novel methodology to reinforce ultrahigh molecular weight polyethylene with carbon nanotubes and a second phase polymer (nylon 6) is presented. The process involves solution spinning followed by melt extrusion, and can be employed to any polyethylene based polymers.
2. The study has demonstrated that dual inclusion of an inorganic (SWCNT) and an organic phase (nylon 6) into UHMWPE is highly effective in enhancing strength, modulus, and most importantly, fracture strain. Improvement in these properties with respect to neat filament was 103%, 219%, and 108%, respectively.
3. As three basic properties, i.e., modulus, strength and fracture strain increased, so did the fracture toughness (u_t) and the elastic energy storage capacity ($\sqrt[3]{\Omega}$) of the fiber since the change in density was insignificant after the reinforcement. The enhancement in toughness and elastic energy was 441% and 88%, respectively.

4. DSC and XRD tests revealed that there is a modest increase in crystallinity, rate of crystallization and crystallite size with SWCNT reinforcement. However, with the addition of nylon 6 these parameters changed significantly because of the increase in the intercrystalline amorphous segment in the three phase system (UHMWPE-SWCNT-nylon 6).
5. SEM micrographs showed that minor polymer phases (nylon-6) were formed as microdroplets, and elongated when load was applied allowing large deformation. Nanotubes were covered with densely packed polymer crystals which was capable of effectively transferring the load to the nanotubes. During plastic deformation stage, polymer slippage allowed elongation while nanotubes carried the load transmitted through the interface.

5. REFERENCES

1. Jacobs, M.J.N., Van Dingenen, L.J., 2001, "Ballistic Protection Mechanisms in personal armor", J Mater Sci 36: 3137-3142.
2. Grujicic, M., Glomski, P.S., He T, Arakere G., Bell, W.C., Cheeseman, B. A. 2009, "Material Modeling and Ballistic Resistance Analysis of Armor-Grade Composites Reinforced with High-Performance Fibers", J Mater Eng Perf 18: 1169-1182
3. Phoenix, S.L., Porwal, P.K., 2003, "A new membrane model for ballistic impact response and V 50 performance of multi-ply fibrous systems", Int J Solid Struct 40: 6723-6765
4. Cooper, C.A., Ravich, D., Lips, D., Mayer, J., Wagner, H.D., 2002, "Distribution and alignment of carbon nanotubes and nanofibrils in a polymeric matrix", Comp Sci Tech 62: 1105-1112
5. Wu, C.L., Zhang, M.Q., Rong, M.Z., and Friedrich, K., 2002, "Tensile performance Improvement of low nanoparticles filled-polypropylene composites", Comp Sci Tech 62: 1327-1341.
6. Runa, S., Gao, P., and Yu, T.X., 2006, "Ultra-strong gel-spun UHMWPE fibers reinforced using multiwalled carbon nanotubes", Poly 47: 1604
7. Runa, S., Gao, P., Yu, T.X., 2003, "Toughening high performance ultrahigh molecular weight polyethylene using multiwalled carbon nanotubes", Poly 44 : 5643
8. Mahfuz, H., Adnan, A., Rangari, V. K., Jeelani, S., 2004, "Carbon Nanoparticles/ Whiskers Reinforced Composites and their Tensile Response", Comp Part A: App Scie Manu, 35: 519-527.
9. Mahfuz, H., Adnan, A., Rangari, V.K., and Jeelani, S., 2005, "Manufacturing and Characterization of carbon nanotube/ polyethylene composites", Int Jour of Nanoscie 4(1): 55
10. Mahfuz, H., Adnan, A., Rangari, V.K., Jeelan, S., Hassan, M.M., Wright, W.J., Deteresa, S.J., 2006, "Enhancement of strength and stiffness of nylon 6 filaments through carbon nanotubes reinforcement", App Phy Lett 88: 083119.

11. Khan, M. R., Mahfuz, H., Leventouri, Th., Rangari, V. K., Kyriacou, A., 2011, "Enhancing toughness of low-density polyethylene filaments through infusion of multiwalled carbon nanotubes and ultrahigh molecular weight polyethylene", *Poly Eng Sci* 51(4): 654-662
12. Mahfuz, H., Khan, M.R., Leventouri, Th., and Liarokapis, E., 2011, "Investigation of MWCNT Reinforcement on the Strain Hardening Behavior of Ultrahigh Molecular Weight Polyethylene", *J Nanotech.* Article ID 637395 : doi:10.1155/2011/637395
13. Miri, V., Persyn, O., Lefebvre, J.M., Seguela, R., 2009, "Effect of Water absorption on the plastic deformation behavior of Nylon 6", *Euro Poly J* 45: 757-762
14. Favis, B.D., 1990, "The effect of processing parameters on the morphology of an immiscible binary blend", *J Appl Poly Sci* 39: 285
15. Bunn, C.W., 1961, "Chemical crystallography an introduction to optical and X-Ray Methods. New York", Oxford University Press,
16. Jenkins, R., and Synder, R.L., 1996 *Introduction to X-Ray powder diffractometry*", New York: John Wiley & Sons. Inc
17. McCarthy, B., Coleman, J.N., Curran, S.A., Dalton, A.B., Davey, A.P., Konya, Z., Fonseca, A., Nagy, J. B., and Blau, W.J., 2000, "Observation of site selective binding in a polymer nanotube composite", *J Mat sci lett* 19: 2239-2241.
18. Mahfuz, H., Hassan, M.M., Dhanak, Beamson, V.G., Stewart, J., Rangari, V., Wei, X., Khabashesku, V., Jeelani, S., 2008, "Reinforcement of nylon 6 with functionalized silica nanoparticles for enhanced tensile strength and modulus", *Nanotec* 19: 445702
19. Hasan, M., Zhou, Y., Mahfuz, H., and Jeelani, S (2006) Effect of SiO₂ nanoparticle on thermal and tensile behavior of nylon-6", *Mat Sci Eng* 429:181.

6. MAILING ADDRESS

Hassan Mahfuz

Ocean & Mechanical Engineering Department,
 Florida Atlantic University,
 Boca Raton, FL 33431
 Email: hmahfuz@fau.edu